Immunity, Vol. 16, 205–218, February, 2002, Copyright ©2002 by Cell Press

Role for CCR7 Ligands in the Emigration of Newly Generated T Lymphocytes from the Neonatal Thymus

Tomoo Ueno,[1] Kyoko Hara,[1] Melissa Swope Willis,[2] Mark A. Malin,[3] Uta E. Höpken,[4] Daniel H.D. Gray,[3] Kouji Matsushima,[5] Martin Lipp,[4] Timothy A. Springer,[2] Richard L. Boyd,[3] Osamu Yoshie,[6] and Yousuke Takahama[1,7]

[1]Division of Experimental Immunology
Institute for Genome Research
The University of Tokushima and
Laboratory of Immune System Development
RIKEN Research Center for Allergy and Immunology
3-18-15 Kuramoto, Tokushima 770-8503
Japan

[2]Center for Blood Research
Harvard Medical School
200 Longwood Avenue
Boston, Massachusetts 02115

[3]Department of Pathology and Immunology
Monash University Medical School
Commercial Road
Prahran 3181, Victoria
Australia

[4]Department of Molecular Tumorgenetics and Immunogenetics
Max-Delbrueck-Center for Molecular Medicine
Robert-Roessle-Strasse 10
Berlin
Germany

[5]Department of Molecular Preventive Medicine
School of Medicine
The University of Tokyo, 7-3-1 Hongo
Tokyo 113-0033

[6]Department of Microbiology
Kinki University Medical School
Osaka 589-0014
Japan

Summary

Most T lymphocytes are generated within the thymus. It is unclear, however, how newly generated T cells relocate out of the thymus to the circulation. The present study shows that a CC chemokine CCL19 attracts mature T cells out of the fetal thymus organ culture. Another CC chemokine CCL21, which shares CCR7 with CCL19 but has a unique C-terminal extension containing positively charged amino acids, failed to show involvement in thymic emigration. Neonatal appearance of circulating T cells was defective in CCL19-neutralized mice as well as in CCR7-deficient mice but not in CCL21-neutralized mice. In the thymus, CCL19 is predominantly localized in the medulla including endothelial venules. These results indicate a CCL19- and CCR7-dependent pathway of thymic emigration, which represents a major pathway of neonatal T cell export.

[7]Correspondence: takahama@genome.tokushima-u.ac.jp

Introduction

The development of T lymphocytes involves dynamic cellular movement of developing lymphocytes through the thymus. Lymphoid precursor cells that are capable of generating T cells immigrate into the thymus from hematopoietic organs such as fetal liver and bone marrow (Fontaine-Perus et al., 1981; Scollay et al., 1986; Jotereau et al., 1987; Dunon and Imhof, 1993; Wilkinson et al., 1999). Within the thymus, developing thymocytes migrate through the cortex to the medulla (van Ewijk, 1991; Picker and Siegelman, 1999). Newly matured T cells emigrate out of the thymus to peripheral lymphoid tissues (Scollay et al., 1980; Scollay and Godfrey, 1995).

Recent studies have shown that chemokine signals may control T cell migration through the thymus. For example, a CXC chemokine CXCL12 (also called stromal cell-derived factor-1, or SDF-1) predominantly attracts immature $CD4^-CD8^-$ and $CD4^+CD8^+$ thymocytes that express the CXCL12 receptor, CXCR4 (Kim et al., 1998; Suzuki et al., 1998). A CC chemokine CCL25 (thymus-expressed chemokine, or TECK) predominantly attracts $CD4^+CD8^+$ thymocytes by binding the receptor CCR9 (Wurbel et al., 2000; Norment et al., 2000). Another CC chemokine CCL22 (macrophage-derived chemokine, or MDC) selectively attracts transitional thymocytes between the $CD4^+CD8^+$ and $CD4^+CD8^-/CD4^-CD8^+$ single-positive (SP) stages by binding CCR4 (Campbell et al., 1999). Mature $CD4^+CD8^-/CD4^-CD8^+$ SP thymocytes efficiently respond to the CCR7 ligands (Kim et al., 1998; Campbell et al., 1999), CCL19 (also known as ELC, MIP-3β, and Exodus-3) (Yoshida et al., 1997; Rossi et al., 1997; Rossi and Zlotnik, 2000) and CCL21 (also known as 6Ckine, Exodus-2, TCA-4, and secondary lymphoid chemokine, or SLC) (Nagira et al., 1997; Tanabe et al., 1997; Hedrick and Zlotnik, 1997). These results indicate that the responsiveness of developing thymocytes to various chemokines sequentially changes during T cell differentiation. However, it is unclear whether and how these chemokines are involved in physiological movement of developing thymocytes through the thymus.

It is interesting to note that transgenic mice expressing the catalytic subunit of pertussis toxin in thymocytes exhibited accumulation of mature T cells in the thymus and failure of T cells to populate peripheral lymphoid organs (Chaffin and Perlmutter, 1991). These results suggested that a pertussis toxin-sensitive G protein-mediated signal is essential for the emigration of mature T cells from the thymus. Since chemokine signals are mediated through pertussis toxin-sensitive G protein-coupled receptors (Murphy, 1994; Cyster and Goodnow, 1995; Premack and Schall, 1996; Cyster, 1999), it is possible that G protein-mediated chemokine signals may be required for thymocyte emigration.

The present study has examined the role of chemokines in the emigration of newly matured T cells out of the thymus. To do so, we have devised a novel technique in which fetal thymus organ culture (FTOC) can be time-lapse visualized under a microscope. We find that, among various chemokines, CCL19 attracts mature

T cells out of the FTOC. In contrast, CCL21, which shares CCR7 with CCL19 (Cyster, 1999; Birkenbach et al., 1993; Yoshida et al., 1998), failed to promote thymocyte emigration. Importantly, either targeted disruption of CCR7 gene or antibody neutralization of CCL19, but not neutralization of CCL21, caused a significant decrease of peripheral circulating T cells in newborn mice, while these mice exhibited an elevation in thymocyte numbers, suggesting that CCR7 and its ligand CCL19, rather than CCL21, are essential for neonatal emigration of most T cells from the thymus in vivo. Confocal immunofluorescence analysis, in situ hybridization analysis, and mRNA analysis of isolated thymic stromal cells indicated that CCL19 is present at higher levels in the medulla than in the cortex, and that most endothelial venules in the medulla are positive for CCL19, suggesting that CCL19 in the medulla attracts mature T cells generated within the thymus, guiding thymic emigration through the venules. These results show that CCL19, rather than CCL21, plays a major role in the emigration of mature thymocytes in newborn mice.

Results

CCL19 Promotes the Emigration of Mature T Cells from Fetal Thymus Organ Cultures

To analyze the role of chemokines in influencing T cell migration through the thymus, we initially tested the effects of adding various chemokines into fetal thymus organ cultures. Among the chemokines tested, we found that addition of the CC chemokine CCL19 (also known as ELC, MIP-3β, and Exodus-3) significantly increased the number of cells found outside of the thymus lobes in the culture medium (Figure 1A). In addition to the chemokines listed in Figure 1A, CCL1, CCL2, CCL3, CCL4, CCL8, CCL11, CCL20, CCL27, XCL1, and CX3CL1 failed to increase the cell number outside of the lobes (data not shown). The extrathymic cells in CCL19-treated cultures were mostly $CD4^+CD8^-$ or $CD4^-CD8^+$ single-positive (SP) TCR-β^{high} mature T cells (Figure 1B), indicating that the cell increase was not due to nonspecific leakage of thymocytes. Most extrathymic T cells were small and $CD25^-CD69^-$, with increased expression of Ly-6A and decreased ability to incorporate bromodeoxyuridine (Figure 1C), therefore resembling physiological, noncycling recent thymic emigrants (Tough and Sprent, 1994; Berzins et al., 1998) rather than extensively proliferating T cells derived from small numbers of artifactually released thymocytes. Thus, the CCL19-induced increase of T cells outside of FTOC lobes was likely due to selective emigration of mature T cells from the thymus.

To directly examine whether CCL19 induces the emigration of mature T cells out of the thymus, we devised a time-lapse FTOC visualization system in which cell movement was directly monitored under the microscope and recorded using a digital CCD camera (Figure 1D). To perform FTOC in transparent culture condition, thymus lobes were submerged in culture medium and maintained in 75% O_2 and 5% CO_2. Thymus cultures were placed in a collagen gel to minimize liquid swirling during culture. An aliquot of CCL19 was spotted into the gel, and the cultures were monitored under the microscope by time-lapse digital recording for 1 day (Figure 1D). As shown in Figure 1E and attached Supplemental Movies (S1 [http://www.immunity.com/cgi/content/full/16/2/205/DC1] versus S2 [http://www.immunity.com/cgi/content/full/16/2/205/DC1] and S3 [http://www.immunity.com/cgi/content/full/16/2/205/DC1]), many cells in the thymus were attracted toward the spot of CCL19 within 1 day in culture. The thymus emigrants in this culture condition were mostly mature T cells (data not shown). Emigrating cells moved specifically toward the CCL19 spot, since no cell migration was observed toward the opposite side of the thymus (Figure 1E; Supplemental Movie S4 at http://www.immunity.com/cgi/content/full/16/2/205/DC1). These results directly indicate that CCL19 attracts mature T cells out of the fetal thymus organ culture.

CCL21 Fails to Mediate the Emigration of Mature T Cells out of the Thymus Culture

Both CCL19 and its CC chemokine family member CCL21 (also known as SLC, 6Ckine, TCA-4, and Exodus-2) interact with the cellular receptor CCR7 (Yoshida et al., 1997, 1998). Unlike CCL19, however, CCL21 failed to mediate the emigration of mature T cells out of the thymus lobes (Figures 1A and 1E; Supplemental Movie S5 at http://www.immunity.com/cgi/content/full/16/2/205/DC1). Titration of CCL19 and CCL21 confirmed that CCL21 is markedly less effective than CCL19 in attracting T cells from the thymus culture (Figure 2A). The selective activity of CCL19 in attracting T cells out of the thymus was also observed in the thymus culture without a collagen-sponge or collagen-gel (data not shown), ruling out the possibility that the selective inefficiency of CCL21 might be due to its adherence to collagen in culture. Thus, the selective emigration-stimulating activity by CCL19 could have been caused by (1) a CCL19-specific signaling pathway that fails to transduce CCL21-derived signals in thymic T cells, and/or (2) a CCL19-specific accessibility to T cells in the fetal thymus lobes. RT-PCR analysis indicated that CCL19-induced thymus emigrants expressed CCR7 (Figure 2B). We also found that CCL19 and CCL21 equivalently induced the chemotaxis of mature SP thymocytes in suspension cultures (Figure 2A). Thus, the failure of CCL21 to attract T cells out of the thymus is apparently not due to a lack of CCR7 or other signaling molecules that transmit CCL21-induced chemotaxis in newly generated T cells. On the other hand, unlike CCL19, CCL21 contains a unique C-terminal extension of amino acids with two cysteine residues and a net positive charge (Nagira et al., 1997; Tanabe et al., 1997; Hedrick and Zlotnik, 1997) (Figure 2C), so that CCL21 may better adhere to negatively charged extracellular matrix components such as heparin-like glycosaminoglycans, rendering CCL21 incapable of entering the thymus organ. Indeed, CCL21 but not CCL19 efficiently bound to heparin, while truncation of the C-terminal extension from CCL21 markedly reduced the heparin binding activity (Figure 2C). The truncated CCL21 considerably gained the ability to attract T cell emigrants out of the thymus (Figure 2D; Supplemental Movie S6 [http://www.immunity.com/cgi/content/full/16/2/205/DC1] versus S7 [http://www.immunity.com/cgi/content/full/16/2/205/DC1]), even

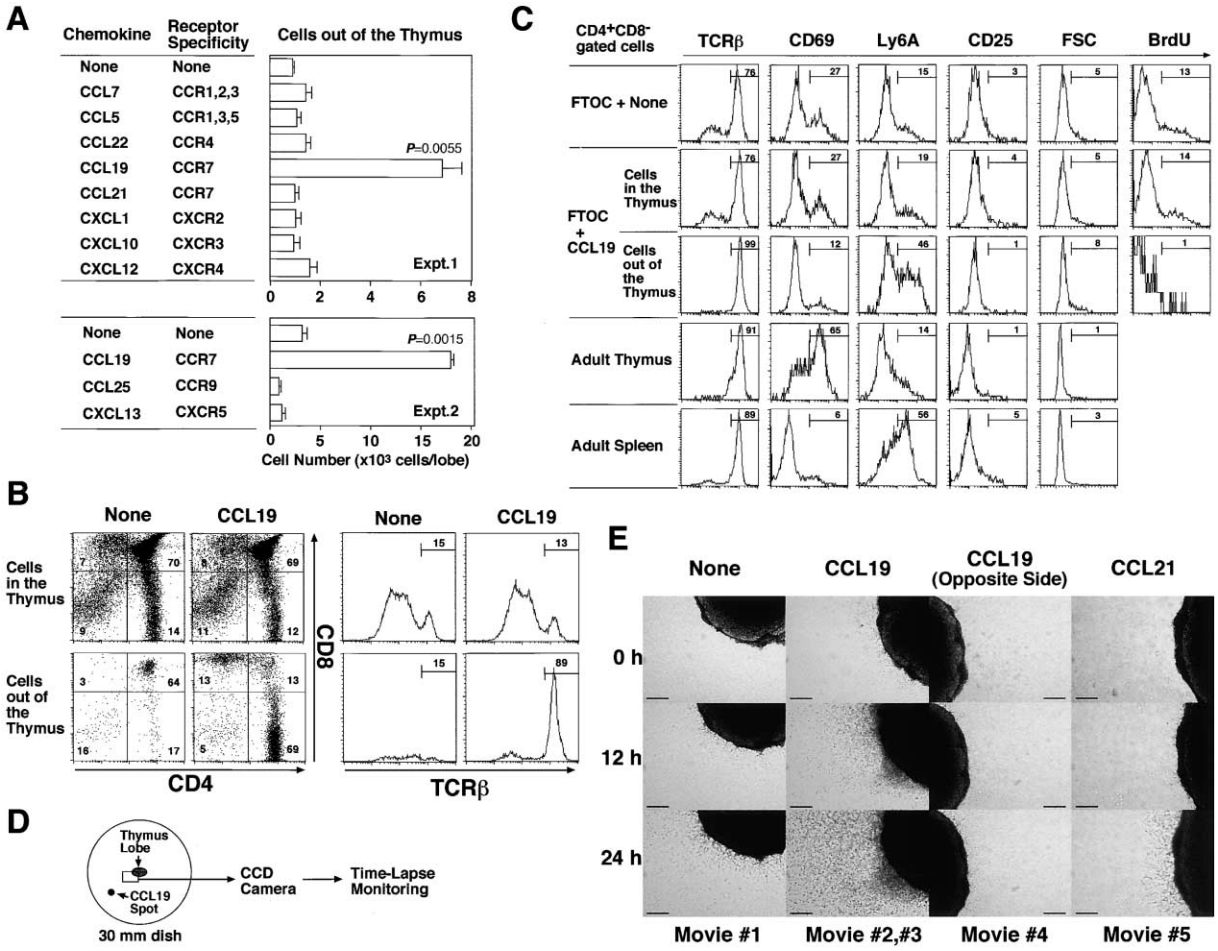

Figure 1. CCL19 Promotes the Emigration of T Cells out of Thymus Lobes

(A) Numbers of cells outside of thymus lobes in culture media supplemented with various chemokines. Mouse fetal thymus lobes were precultured for 5 to 10 days, so that the thymus organs contained thymocytes in a broad range of developmental stages, resembling the distribution of mature adult thymus. FTOC thymus lobes were washed and cultured for an additional 2 days in the absence or presence of indicated chemokines at 100 nM. Listed are means and standard errors (n = 4–9) of viable cell numbers found outside of the thymus lobes 2 days after adding chemokines. Significance (*P*-value) of the cell numbers over the culture condition in the absence of chemokines was evaluated by Student's t test using StatView software (SAS Institute Inc., Cary, NC).

(B) Flow cytometric analysis of cells in FTOC cultures in the absence or presence of CCL19. Cells were 3-color stained for CD4, CD8, and TCR-β. Numbers within each area indicate the frequency of cells within that area.

(C) Flow cytometric analysis of $CD4^+CD8^-$ cells in the FTOC cultures containing CCL19. Cells were 3-color stained for CD4, CD8, and indicated molecules. Surface levels of indicated molecules and forward light scatter (FSC) intensity, which estimates cell size, were measured for the $CD4^+CD8^-$ gated cells. FTOC cells were also assessed for DNA synthesis during the last 4 hr of culture by intracellular staining of bromodeoxyuridine (BrdU) incorporation.

(D) A diagram of the time-lapse FTOC visualization system employed to monitor cellular movement out of the thymus. An FTOC lobe was placed in a transparent collagen gel and cultured in medium under high oxygen conditions. Either 10 μM CCL19 or 10 μM CCL21 (5 μl) was spotted into a collagen gel approximately 10 mm outside of the thymus lobe. The culture within the rectangular box was time-lapse monitored under the microscope with a CCD camera for 24 hr.

(E) FTOC visualized at indicated time points after spotting CCL19 or CCL21. Where indicated, the thymus lobe was monitored on the opposite side of the CCL19 spot, indicating that cell emigration was directed toward the CCL19 spot. Bar, 250 μm. Animated versions of the pictures are shown as QuickTime files (Supplemental Movies S1–S5 at http://www.immunity.com/cgi/content/full/16/2/205/DC1). Representative results of ≥10 (B), 2–3 (C), and ≥4 (E) independent experiments are shown.

though truncated CCL21 in suspension culture exhibited a slightly decreased chemotactic activity (Figure 2D). Moreover, binding assay of ^{125}I-labeled proteins directly showed that CCL19 exhibited better access to T cells in the intact thymus organ rather than CCL21 (Figure 2E). These results suggest that the inefficient activity of CCL21 to attract T cells from the thymus is at least in part due to the limited ability of CCL21 to diffuse into the organ. Thus, unlike CCL19, CCL21 is inefficient in stimulating thymic emigration in fetal thymus organ culture.

Defective Thymic Emigration in CCR7-Deficient Newborn Mice

We then wished to examine the in vivo roles for CCL19 and CCL21 in thymic emigration. In newborn mice, thy-

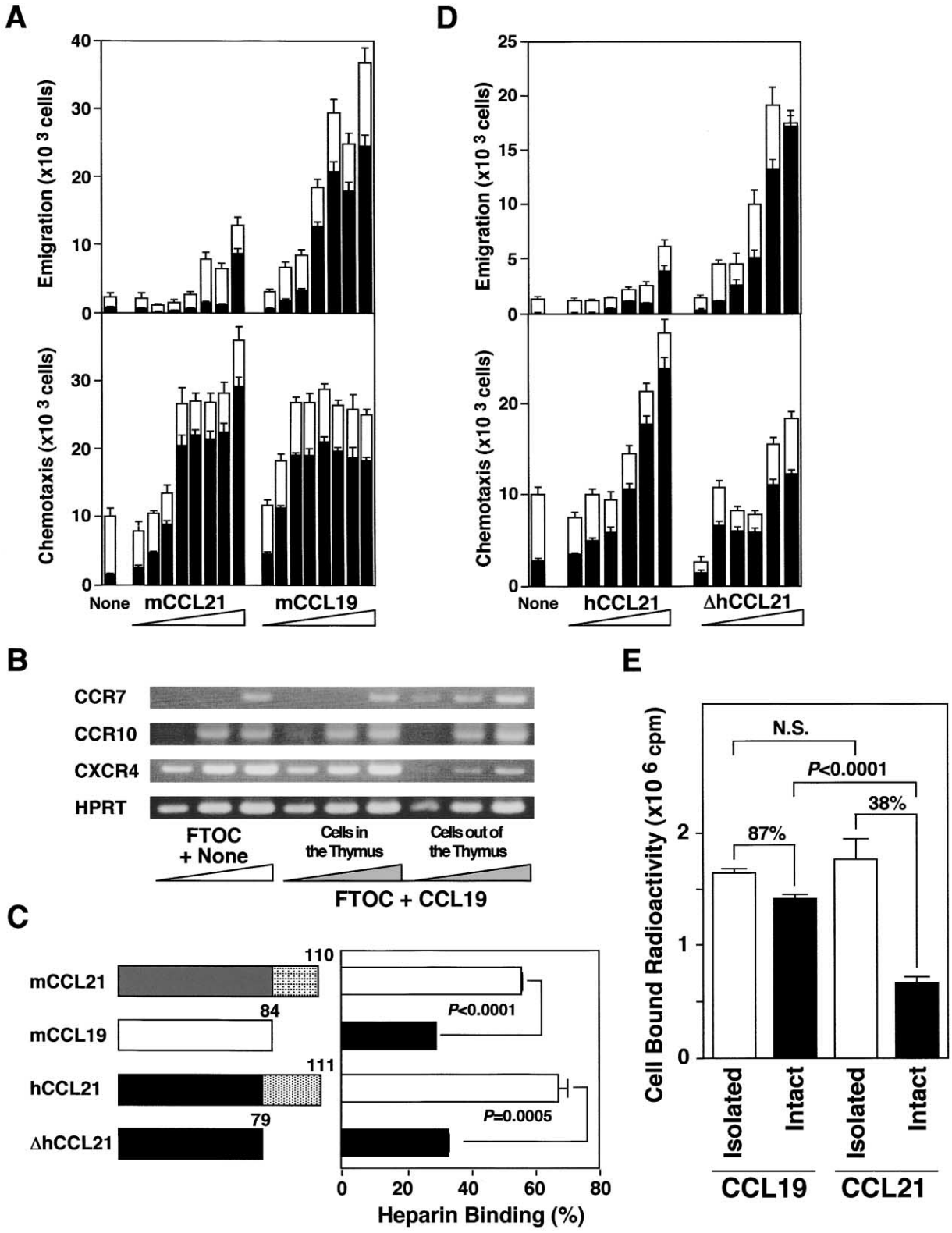

Figure 2. The Role of CCL19 and CCL21 in the Thymic Emigration and T Cell Chemotaxis In Vitro

(A) CCL19 and CCL21 were examined for their ability to attract mature thymocytes out of thymus lobe (upper panel) (as in Figure 1) and for their chemotaxis activity to attract mature thymocytes in suspension culture (lower panel). Two-fold serial dilutions (in the range of 1.56 nM to 200 nM) of recombinant mouse CCL21 and CCL19 proteins (R&D Systems) were examined. Means and standard errors (n = 4–8) of viable cell numbers of total migrated cells (total height of the bars) and TCR-β^{high} mature T cells (filled bars) are indicated.

(B) Reverse transcriptase-PCR analysis for mRNA levels of CCR7 in CCL19-reactive thymus emigrants. Serial dilutions of cDNA from indicated

mic emigrants of mature T cells begin to populate peripheral lymphoid organs including the spleen (Figure 3A). Neonatal supply of spleen T cells detected by 5 days old is completely absent in *nu/nu* mice lacking the thymus (Figure 3A), suggesting that neonatal T cells in the spleen are derived from the thymus, representing recent thymic emigrants. Interestingly, we found that newborn T cells in the spleen of CCR7-deficient mice (Förster et al., 1999) were markedly lower in number than those of wild-type mice (Figure 3A). T cell number in CCR7-deficient mice was lower not only in the white pulp area but also in the red pulp area of the spleen (Figures 3B and 3C), into which lymphocytes enter along the blood flow without active migration through pertussis-toxin-sensitive chemokine signals (Cyster and Goodnow, 1995), suggesting that T cell number in open blood circulation is lower in CCR7-deficient neonates than wild-type neonates. On the other hand, thymocytes in neonatal CCR7-deficient mice were slightly but significantly higher in number than those in age-matched wild-type mice (Figure 3A). These results suggest that the neonatal supply of T cells from the thymus to the circulation is greatly reduced in CCR7-deficient mice, and that CCR7 is essential for neonatal emigration of most T cells from the thymus.

It should be noted that, in the absence of CCR7, a small number of T cells were found in newborn spleen (Figure 3A) and T cell number in adult spleen was even higher in CCR7-knockout mice than in control mice (Figure 3D), suggesting that thymic emigration can occur independently of CCR7 as a minor pathway during the neonatal period. It is possible that the CCR7-independent thymic emigration becomes a major pathway in adult mice, or that a small number of CCR7-independent thymic emigrants expands during postnatal period to saturate the peripheral tissues in adult mice.

CCL19 Neutralization Impairs Thymic Emigration of Neonatal T Cells In Vivo

To further examine the role of CCL19 and CCL21 in thymic emigration in vivo, normal newborn mice were injected daily with either anti-CCL19 or anti-CCL21 neutralizing antibodies, which specifically blocked the chemotaxis of thymocytes toward CCL19 and CCL21, respectively (Figure 4A). We found that administration of anti-CCL19 neutralizing antibody significantly inhibited the supply of spleen T cells as well as circulating peripheral blood T cells (Figures 4B–4D). At 3 days old, the number of thymocytes in anti-CCL19-treated mice was slightly but significantly higher than in the control antibody-treated mice (Figure 4B). On the other hand, the injection of anti-CCL21 neutralizing antibody did not significantly affect the numbers of spleen T cells or thymocytes in neonatal mice (Figures 4B–4D). Anti-CCL21 antibody, however, significantly inhibited the supply of T cells to lymph nodes (Figure 4D) as expected from previous studies (Gunn et al., 1998; Stein et al., 2000), suggesting that the injected anti-CCL21 antibody maintained its in vivo neutralizing activity to CCL21, inhibiting T cell migration to lymph nodes. These results suggest that in vivo neutralization of CCL19, but not CCL21, impaired thymic emigration of T cells to peripheral circulation. Thus, our results suggest that CCL19 rather than CCL21 plays a major role in neonatal emigration of mature T cells out of the thymus in vivo.

Although it was possible that mature single-positive thymocytes might accumulate in either CCR7-deficient or CCL19-neutralized mice, we have so far detected no difference in expression profiles of CD4, CD8, and TCR in neonatal thymocytes among normal, CCR7-deficient, and CCL19-neutralized mice (data not shown).

Expression of CCL19 in the Mouse Thymus

Finally, we have examined the localization of CCL19 within the thymus by immunofluorescence analysis. In secondary lymphoid organs, CCL19 is mainly produced by dendritic cells as well as T zone stromal cells (Ngo et al., 1998; Luther et al., 2000). Consistent with previous reports (Annunziato et al., 2000), CCL19 in the adult thymus was predominantly detected in the MTS10$^+$ medulla rather than in the CDR1$^+$ cortex (Figures 5A–5F). In the medulla, CCL19 was localized to MTS10$^+$ epithelial cells, CD11c$^+$ dendritic cells, as well as CD31$^+$ endothelial venular cells (Figures 5D–5L). Importantly, most CD31$^+$ venules in the medulla were positive for CCL19 (Figures 5J–5O). Also in the newborn thymus, CCL19 immunofluorescence signals were predominantly detected within the G8.8^{high} medullary area (Figures 6A–6C),

cells were PCR-amplified for CCR7, CCR10, and CXCR4. The thymic emigrants expressed CCR7 at levels higher than the cells that remained in the thymus, whereas the expression of CXCR4 was lower in the emigrants than in the thymocytes. Housekeeping HPRT levels and other chemokine receptor CCR10 levels were approximately equivalent among the cells. Representative results of ≥2 independent experiments are shown.

(C) Heparin binding abilities of mouse CCL21 (mCCL21), mouse CCL19 (mCCL19), human CCL21 (hCCL21), and a truncated mutant form of hCCL21 (ΔhCCL21). Numbers above the schematic representation of the chemokines indicate amino acid numbers of indicated proteins. Dotted regions of CCL21 indicate the C-terminal extension with a net positive charge. An equal amount of ^{125}I-labeled proteins was incubated with either heparin-agarose gel or control agarose gel, and the gel-bound radioactivity was measured. Means and standard errors (n = 4) of radioactivity specifically bound to heparin are shown.

(D) Recombinant hCCL21 and ΔhCCL21 were examined for their ability in the thymic emigration assay (upper panel) and for the chemotaxis assay in suspension culture (lower panel) as in (A). Two-fold serial dilutions of proteins were made in the range of 100 nM to 3200 nM for the thymic emigration assay and 12.5 nM to 400 nM for the chemotaxis assay. Means and standard errors (n = 4–8) of viable cell numbers are indicated. Animated versions of the pictures can be found as supplementary results (Supplemental Movie S6 [at http://www.immunity.com/cgi/content/full/16/2/205/DC1] for hCCL21 and Supplemental Movie S7 [at http://www.immunity.com/cgi/content/full/16/2/205/DC1] for ΔhCCL21).

(E) Equal amount of ^{125}I-labeled CCL19 or CCL21 was incubated with either an intact FTOC lobe or isolated thymocytes from an FTOC lobe. Thymocytes were isolated, washed, and measured for the bound radioactivity. Means and standard errors (n = 3–5) of radioactivity per thymocytes in one FTOC lobe are indicated.

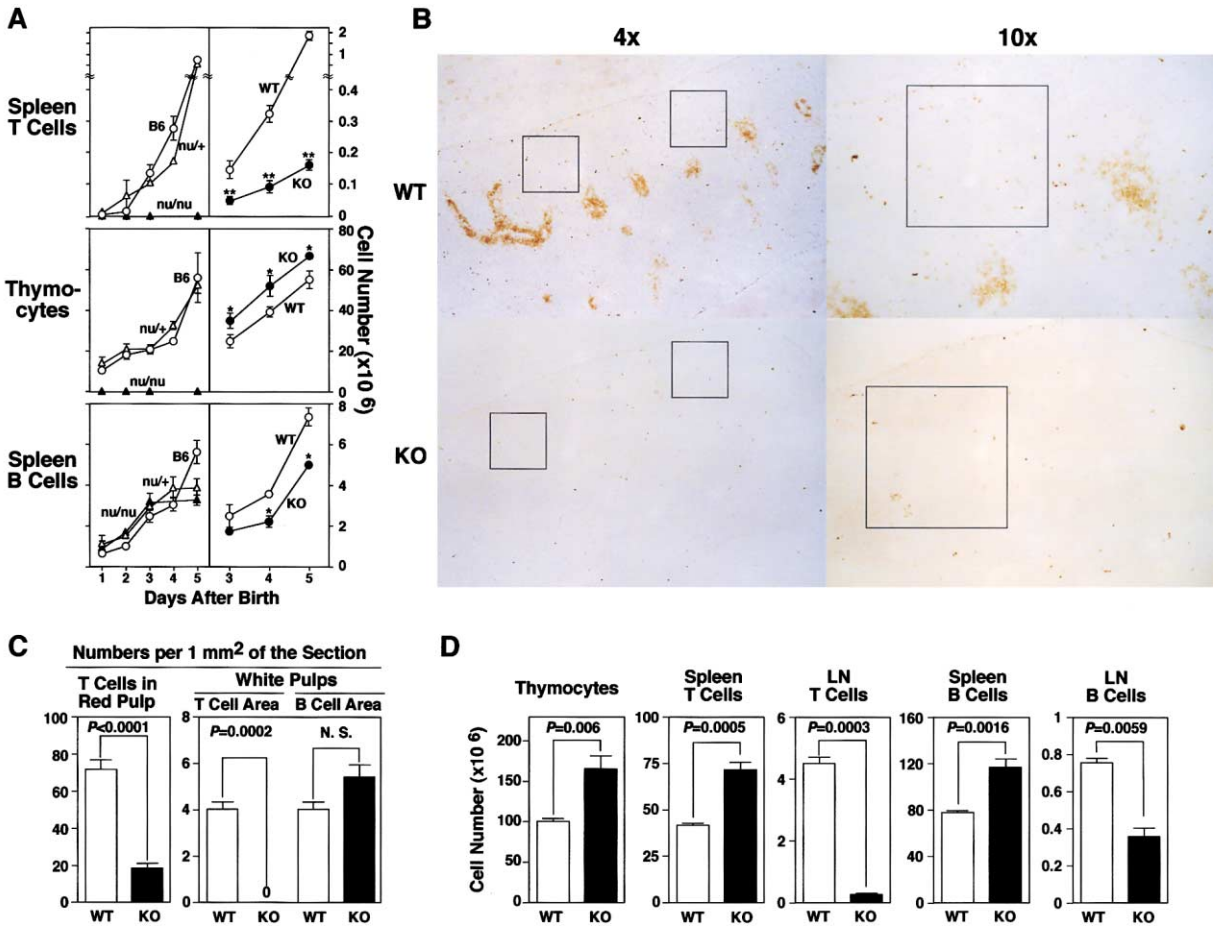

Figure 3. Defective Supply of Peripheral T Cells in CCR7-Deficient Newborn Mice In Vivo

(A) Ontogeny of spleen T cells and B cells in newborn mice at indicated age of days after birth. T and B cells in the spleen were identified as TCR-β^+CD3$^+$ and B220$^+$CD3$^-$ cells, respectively, using flow cytometry. Numbers of total thymocytes are also shown. Results from normal mice (B6, open circles; BALB/c-*nu*/+ mice, open triangles) and thymus-deficient *nu*/*nu* mice (BALB/c-*nu*/*nu*, closed triangles) show that spleen T cells during the neonatal period are virtually all thymus-derived (left panels). Numbers of spleen T cells and thymocytes in CCR7-deficient (KO, closed circles) and wild-type mice (WT, open circles) show that numbers of spleen T cells and thymocytes are significantly (*$P < 0.05$; **$P < 0.005$) lower and higher in CCR7-deficient mice than in wild-type mice, respectively (right panels).

(B and C) Immunohistochemical analysis of 5-day-old spleens from CCR7-deficient and wild-type mice. Representative sections stained for T cells (Thy-1.2) are shown. Boxes indicate 0.25 mm^2 red pulp areas identified by the Thy-1 and B220 staining profiles of serial sections. Indicated in (C) are means and standard errors of T cell numbers in the red pulp area (n = 10) and of the numbers of white pulp areas (n = 5) per 1 mm^2 of the section. In addition to the loss of T cell areas in the white pulp, the number of T cells in the red pulp area was significantly lower in CCR7-deficient mice than wild-type mice.

(D) Distribution of lymphocytes in adult CCR7-KO and WT mice (9 weeks old). Shown are means and standard errors (n = 3–8 in [A], n = 4–8 in [D]) of viable cell numbers in the spleen, thymus, and inguinal lymph nodes.

and were found in most CD31$^+$ endothelial venular cells but not in MTS15$^+$ fibroblasts (Figures 6D–6F). In situ hybridization analysis of newborn thymus also showed that CCL19 transcripts were weakly detected within the medullary area (Figures 7A–7C), as has been reported (Bleul and Boehm, 2000). Further analysis involved isolation of thymic stromal cell subsets for RT-PCR analysis of CCL19 mRNA expression. As shown in Figure 7E, CCL19 mRNA in the thymus was most highly detected in medullary epithelial cells, rather than endothelial cells, dendritic cells, cortical epithelial cells, or thymocytes. CCL21 mRNA was also mainly expressed by medullary epithelial cells among the four kinds of sorted cell populations. Given the strong signals of CCL21 mRNA in total thymic stromal samples, however, cells other than these four populations might also express CCL21 mRNA. Together, these results indicate that CCL19 in the thymus is predominantly produced by medullary epithelial cells and localized to epithelial cells, dendritic cells, and endothelial cells within the medulla. It is interesting to note that, in double immunofluorescence analysis (Figures 6G–6I), in situ hybridization analysis (Figures 7C and 7D), or RT-PCR analysis (Figure 7E), CCL21 signals were detected in an overlapping population of cells with CCL19 signals but detected in a broader population of cells than CCL19 signals, suggesting that CCL19 and CCL21 may play different, though possibly overlapping, roles in the thymus. These results are consistent with

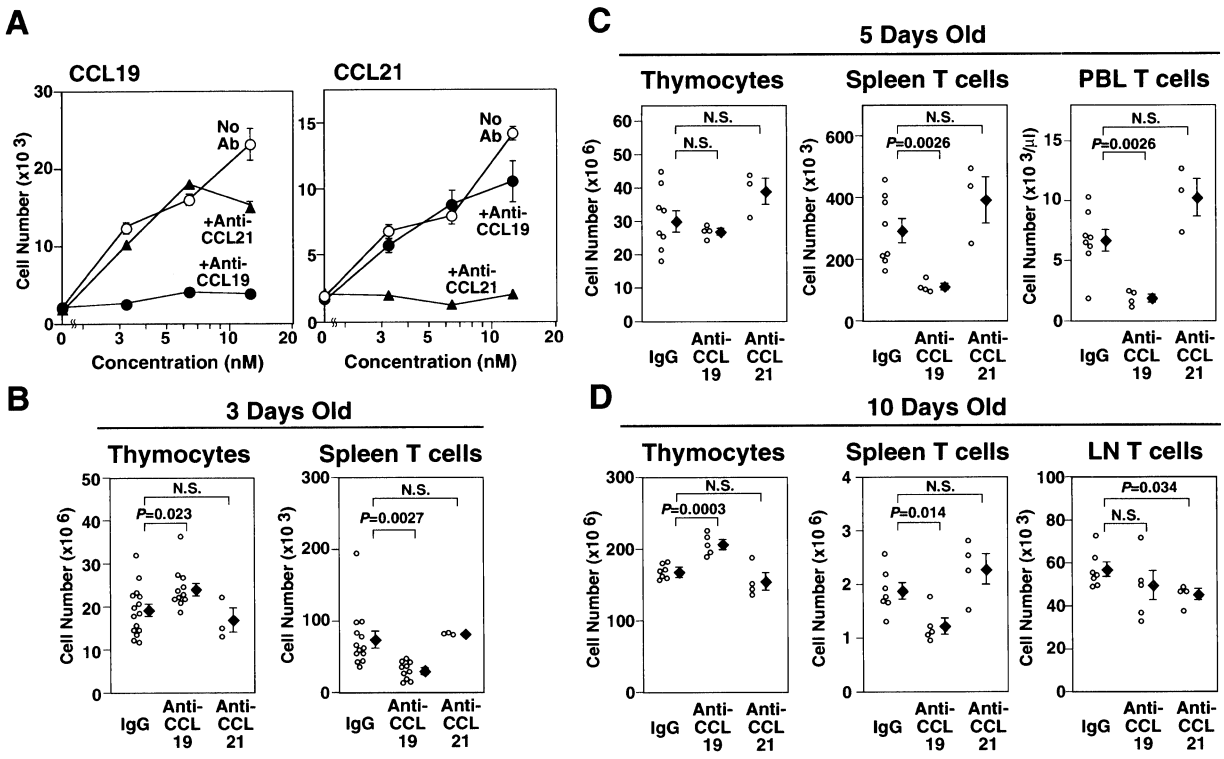

Figure 4. The Effects of Anti-CCL19 and Anti-CCL21 on the Peripheral T Cell Supply in Newborn Mice In Vivo

(A) The specificity of anti-CCL19 and anti-CCL21 neutralizing antibody. Anti-CCL19 or anti-CCL21 goat IgG antibody (10 μg/ml) was added to the chemotaxis assay of thymocytes for CCL19 (left panel) and CCL21 (right panel) in suspension cultures.

(B–D) The effects of in vivo injection of anti-CCL19 antibody or anti-CCL21 antibody in normal newborn mice. Goat antibodies were injected daily, and indicated cells were analyzed on 3 days old (B), 5 days old (C), and 10 days old (D). Independent preparation of rabbit anti-CCL21 antibody similarly affected to the goat anti-CCL21 antibody, in which the numbers of thymocytes and spleen T cells were not affected on day 3, 5, or 10 but the number of lymph node T cells examined on day 10 was reduced (data not shown). Means and standard errors (n = 4 in [A]) of viable cell numbers are indicated. In (B)–(D), open circles represent cell numbers of individual mice examined (n = 3–15).

the possibility that CCL19 in the medulla attracts mature T cells generated within the thymus, guiding thymic emigration through endothelial venules in the medulla.

Discussion

Thymic emigration of newly generated T cells is an essential process for seeding circulating T cells. The present study examined the role of chemokines in the emigration of T cells from the thymus, utilizing a modified fetal thymus organ culture to directly visualize and evaluate the thymocyte emigration. We have found that, among various chemokines tested, only one chemokine, CCL19, attracted mature T cells out of fetal thymus organ cultures. The CCL19-attracted T cells phenotypically resembled recent thymic emigrants. Interestingly, CCL21, which shares a common receptor CCR7 with CCL19, failed to cause thymocyte emigration. Using truncated CCL21, we have found that the failure of CCL21 to mediate thymocyte emigration was at least in part due to its unique C-terminal extension containing positively charged amino acids. By this C-terminal extension, CCL21 efficiently adheres to negatively charged extracellular matrix components such as heparin-like glycosaminoglycans, thereby being inefficient in accessing T cells in the thymus organ. The selective role for CCL19, rather than CCL21, in attracting T cells out of the thymus was further supported by in vivo experiments in which antibody-mediated neutralization of CCL19 but not CCL21 in newborn mice impaired thymic emigration of T cells to the peripheral circulation. In CCL19-neutralized mice and CCR7-deficient mice, but not in CCL21-neutralized mice, circulating T cells were reduced and thymocytes accumulated in the neonates. Our results indicate that CCL19, rather than CCL21, plays a major role in the emigration of mature T cells out of the thymus in newborn mice.

Analysis of CCL19 distribution in adult and newborn mice showed that CCL19 in the thymus is predominantly localized within the medulla. Consistent with a previous report (Bleul and Boehm, 2000), our results show that CCL19 mRNA in the thymus was primarily detected in medullary epithelial cells rather than other stromal cells, including dendritic cells, endothelial cells, and cortical epithelial cells. In the medullary area, however, CCL19 protein was localized to dendritic cells and endothelial cells as well as epithelial cells. Since CCL19 mRNA levels were low in dendritic cells and endothelial cells, it is possible that a fraction of CCL19 localized on these cells may be derived from nearby medullary epithelial cells, a possibility consistent with a recent finding that CCL19 generated in the perivascular stroma is translo-

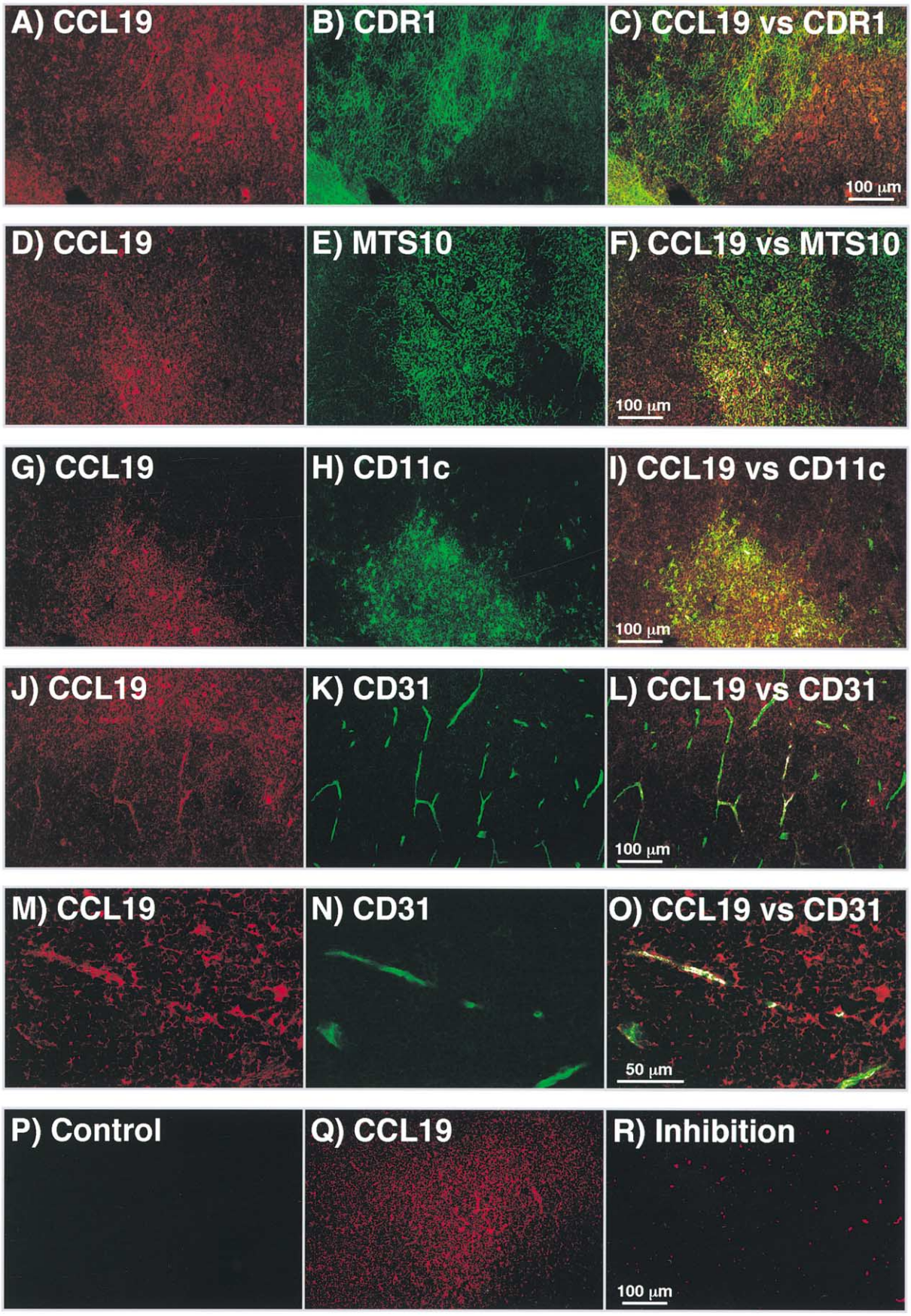
A) CCL19
B) CDR1
C) CCL19 vs CDR1
100 μm
D) CCL19
E) MTS10
F) CCL19 vs MTS10
100 μm
G) CCL19
H) CD11c
I) CCL19 vs CD11c
100 μm
J) CCL19
K) CD31
L) CCL19 vs CD31
100 μm
M) CCL19
N) CD31
O) CCL19 vs CD31
50 μm
P) Control
Q) CCL19
R) Inhibition
100 μm

cated to the high endothelial venules of the secondary lymphoid tissues (Baekkevold et al., 2001). It is further possible that a fraction of CCL19 localized in the thymus may be derived from remote organs, i.e., parathymic lymph nodes, since the thymus organ is highly accessible to CCL19 (Figures 2A and 2E). Nonetheless, it is important to note that CCL19 was found on most endothelial venules in the medulla. A recent report on the analysis of human thymus sections also showed that CCL19 immunoreactivity in the thymus, which was primarily localized to medullary epithelial cells, was often found in cells surrounding medullary vessels (Annunziato et al., 2000). Thus, it is possible that CCL19 may direct mature thymocytes not only to the medullary area but also to endothelial venules within the medulla, through which mature thymocytes may emigrate to the blood circulation. Further mechanisms of thymic emigration, including the mechanism of possible T cell relocation from the tissue side to the lumen side of the vessels, are still unclear.

Our results suggest that, unlike CCL19, CCL21 fails to show a role in thymic emigration. However, like CCL19, CCL21 in the thymus was localized predominantly in the medulla, as has been previously described (Tanabe et al., 1997; Bleul and Boehm, 2000). Our results further show that CCL21 in the thymus is localized in an area that overlaps with CCL19 but is localized in a broader area than CCL19, suggesting that CCL21 in the thymus may play a role that is similar to but is different from CCL19 that is involved in thymic emigration. It is possible that CCL21 may be involved in attracting maturing thymocytes from the cortex to the medulla and that CCL19 may also be involved in this process.

The present results using CCR7-deficient mice clearly document a major involvement of CCR7 in the neonatal seeding of the peripheral T cell pool in vivo. In CCR7-deficient newborn mice, the number of peripheral T cells including the open circulating red pulp T cells was significantly reduced, whereas the number of thymocytes was significantly increased. Antibody-mediated neutralization of CCL19, but not CCL21, caused essentially the same effect on T cell distribution in normal newborn mice, i.e., increased in thymocytes and reduced in peripheral T cells including blood circulating T cells. These results strongly suggest that the chemokine signal through CCR7, most likely mediated by CCL19, plays a key role in the emigration of T cells from the thymus in newborn mice. The greater effect of CCR7 deficiency than the anti-CCL19 treatment in newborn mice could be due to incomplete neutralization of CCL19-CCR7 interaction by the antibody injection, and/or the involvement of unidentified ligands for CCR7 other than CCL19 or CCL21. Importantly, our data along with previous results (Förster et al., 1999) indicate that the number of circulating T cells in adult CCR7-deficient mice is not reduced. Thus, it is logical to assume that thymic emigration can occur via a CCR7-independent pathway in addition to the CCR7-dependent pathway. It is not clear whether the CCR7-independent thymic emigration may represent a major pathway in adult mice, or whether a small number of CCR7-independent neonatal thymic emigrants (as seen in Figure 3) may subsequently expand to saturate the peripheral tissues in adult mice. However, it has been recently shown that there is a continuous supply of thymic emigrants in adult mice (Berzins et al., 1998, 1999) and in adult humans (Douek et al., 1998; Poulin et al., 1999), and that these recent thymic emigrants in adult are involved in maintaining a peripheral pool of T cells with a diverse repertoire (Berzins et al., 1998; Poulin et al., 1999). It is possible that thymic emigration in adult may largely occur via a CCR7-independent pathway, unlike neonatal thymic emigration that is largely CCR7 dependent. It has been also reported in sheep (Miyasaka et al., 1990) and in guinea pig (Kotani et al., 1966) that thymic emigration also occurs via lymphatic drainage in addition to the emigration via blood vessels (Miyasaka et al., 1990). It is thus possible that the CCR7-dependent and CCR7-independent emigration processes may represent either one of the pathways via lymphatic or blood vessels. Interestingly, adult transgenic mice expressing the catalytic subunit of pertussis toxin in thymocytes exhibited accumulation of T cells in the thymus and failure of T cells to populate peripheral lymphoid organs (Chaffin and Perlmutter, 1991). Thus, the CCR7-independent pathway of thymic emigration may still be dependent on pertussis toxin-sensitive signals through G protein-coupled chemokine receptors.

The present study suggests that CCL19 and CCL21, even though they share CCR7, are functionally different in relocating T lymphocytes from the primary lymphoid organ to secondary lymphoid organs. In secondary lymphoid organs, locally produced CCL21 mainly participates in promoting the homing of $CCR7^+$ lymphocytes into the organ through high endothelial venules (Stein et al., 2000; also supported by the results in Figure 4). CCL21 may additionally exhibit a unique role through the CXCR3 receptor, which interacts with CCL21 but does not interact with CCL19 (Soto et al., 1998; Lu et al., 1999). On the other hand, CCL19 in secondary lymphoid organs, which is also involved in homing of $CCR7^+$ lymphocytes via the high endothelial venules (Baekkevold et al., 2001), is suggested to be involved in promoting encounters between recirculating T cells and dendritic cells and in the migration of activated B cells into the T cell zone (Ngo et al., 1998). Our results suggest an

Figure 5. Distribution of CCL19 in the Adult Thymus

Thymus sections from adult B6 mice were stained with biotin-conjugated anti-CCL19 antibody and streptavidin-Alexa-568 (red) and indicated antibodies visualized with Alexa-488 (green). White signals in right panels show colocalization of Alexa-568 signals with Alexa-488 signals. Bars, 100 μm for (A)–(L) and (P)–(R), and 50 μm for (M)–(O). Note that CCL19, enriched in $MTS10^+$ medulla rather than $CDR1^+$ cortex, is colocalized with $MTS10^+$ epithelial cells, $CD11c^{hi+}$ dendritic cells, as well as $CD31^+$ endothelial venules. (L) and (O) indicate that most endothelial venules express CCL19. The CCL19 signals were specific, though not very strong, since (i) the signals were specifically detected by multiple batches of anti-CCL19 antibodies (A)–(O) and (Q) but not by control antibodies (P), (ii) the signals were specifically reduced by preabsorption of the antibody with CCL19 but not with CCL21 (data not shown), and (iii) the signals were specifically reduced by preincubation of the staining reaction with CCL19 (R).

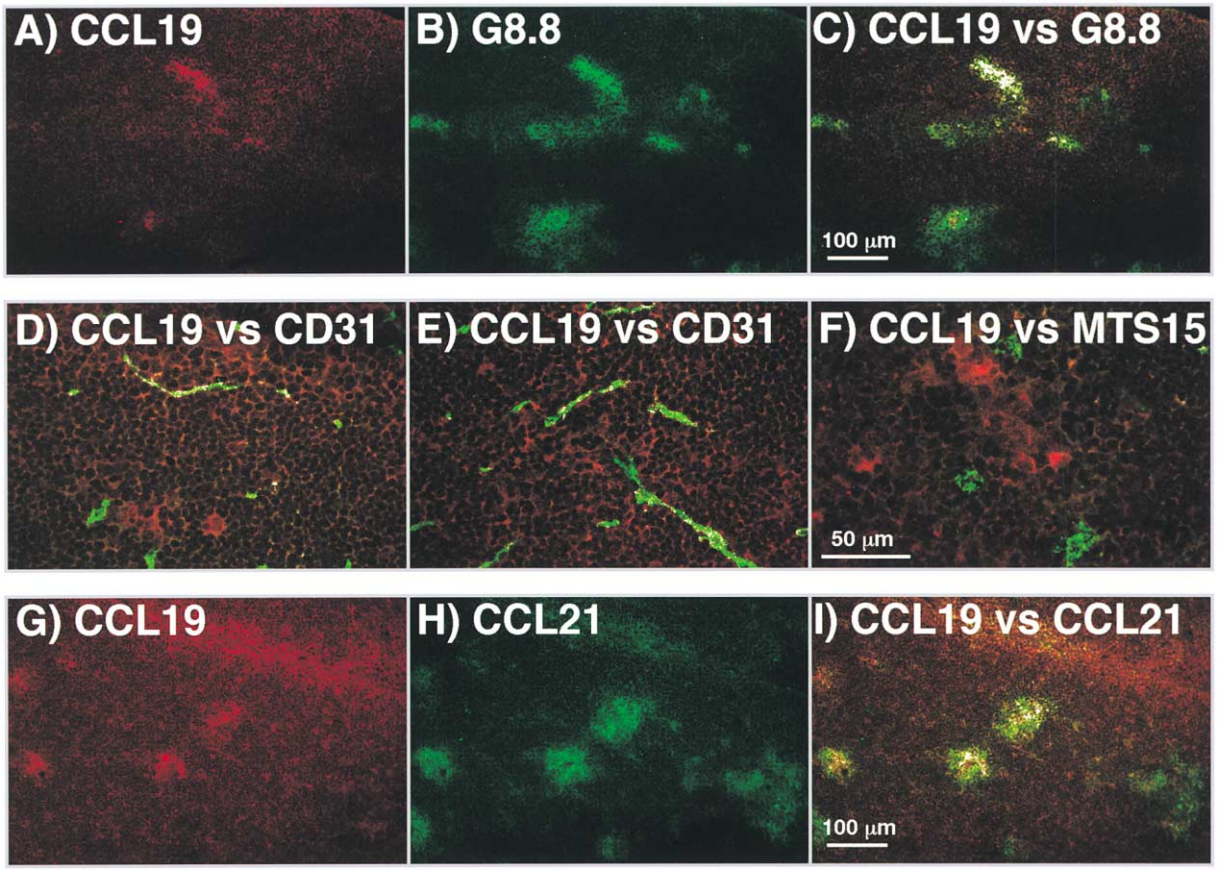

Figure 6. Distribution of CCL19 in the Newborn Thymus

Thymus sections from 3 day old B6 mice were stained with biotin-conjugated anti-CCL19 antibody and streptavidin-Alexa-568 (red) and indicated antibodies visualized with Alexa-488 (green). White signals in (C), (D), (E), (F), and (I) indicate colocalization of Alexa-568 signals with Alexa-488 signals. Bars, 100 μm for (A)–(C) and (G)–(I) and 50 μm for (D)–(F). In the thymus, G8.8^{high} areas identify the medulla (Nelson et al., 1996) and MTS15 expression identifies fibroblasts (Gray et al., 2002).

additional role of CCL19 in lymphocyte traffic, in which CCL19 in the thymic medulla may attract newly generated T lymphocytes by binding to CCR7 receptor and may play a previously unidentified role of chemokine in promoting the emigration of thymus-generated T cells into the circulation. Thus, CCL19 and CCL21 may cooperate in attracting CCR7$^+$ T cells from the thymus to peripheral lymphoid organs, by guiding the emigration of newly generated thymocytes to the circulation and directing the immigration of circulating naive T cells to the secondary lymphoid organs.

Experimental Procedures

Chemokines

Recombinant proteins of mouse CCL1 (TCA3), CCL2 (JE), CCL3 (MIP-1α), CCL4 (MIP-1β), CCL11 (eotaxin), CCL19 (ELC), CCL20 (LARC), CCL21 (SLC), CCL22 (MDC), CCL25 (TECK), CCL27 (CTACK), CXCL12 (SDF1), CXCL13 (BLC), XCL1 (lymphotactin), and CX3CL1 (fractalkine) were obtained from R&D Systems, Minneapolis, MN. Recombinant proteins of mouse CCL5 (RANTES), CCL7 (MCP3), CCL8 (MCP-2), CXCL1 (KC), and CXCL10 (IP10) were obtained from PeproTech, Rocky Hill, NJ.

Truncated CCL21 Protein

Recombinant human CCL21 and truncated CCL21 (amino acids 1-79) were produced using the Pichia pastoris yeast expression system (Invitrogen) following the manufacturer's protocol. The coding sequence of wild-type CCL21 was generated by PCR using the sense primer 5′-GAA**CTCGAG***AAAAGA*AGTGATGGAGGGGCT-3′ containing an XhoI restriction site (in bold), yeast α-secretion factor sequence prior to the Kex2 cleavage site (in italic) and the codons of the first 5 amino acids of human CCL21 (underlined). The antisense primer 5′-ATT**TCTAGA***TGA*GCCCTGGGCTGGTTTCTG-3′ annealed to codons corresponding to amino acids 74-79 (underlined), a stop codon (italic), and an XbaI restriction site (bold). The template for each PCR reaction was PCRII/huSLC (kindly provided by Dr. K. Hieshima). The PCR products were cloned into pPicZαA, transfected into *E. coli* DH5α, and recombinant colonies were selected on plates containing 25 μg/ml zeocin. Plasmid from a single colony of each construct was purified and the sequence of the insert confirmed. Plasmid (10 μg) containing the correct sequence was linearized using PmeI and transfected into GS115 Pichia pastoris using electroporation. Colonies were selected on YPDS plates containing 100 μg/ml zeocin at 30°C for 2–3 days. For large-scale growth and purification, the highest expressing colony was used to inoculate 25 ml of BMGY in a baffle flask and incubated in a 30°C shaking incubator overnight. One liter of BMGY was inoculated with the overnight culture and grown 2 days to an OD_{600} of 10-20. Protein production was initiated by spinning down the culture and resuspending the pellet in 200 ml BMMY containing 1% methanol. Cultures were put back on the 30°C shaker and methanol was added every 24 hr to a final concentration of 1%. After 72 hr, the supernatant was collected, filtered with a 0.22 μm filter, and purified using cation exchange chromatography. Wild-type and mutant CCL21 were ~98% pure as determined by SDS-PAGE and Coomassie staining.

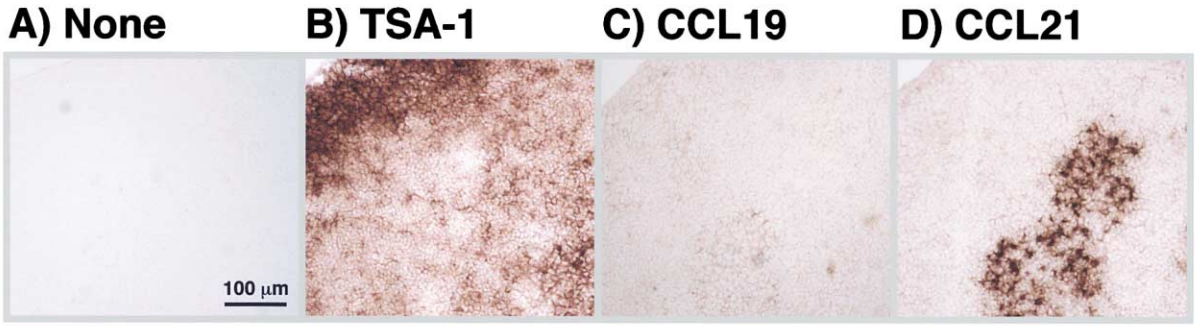

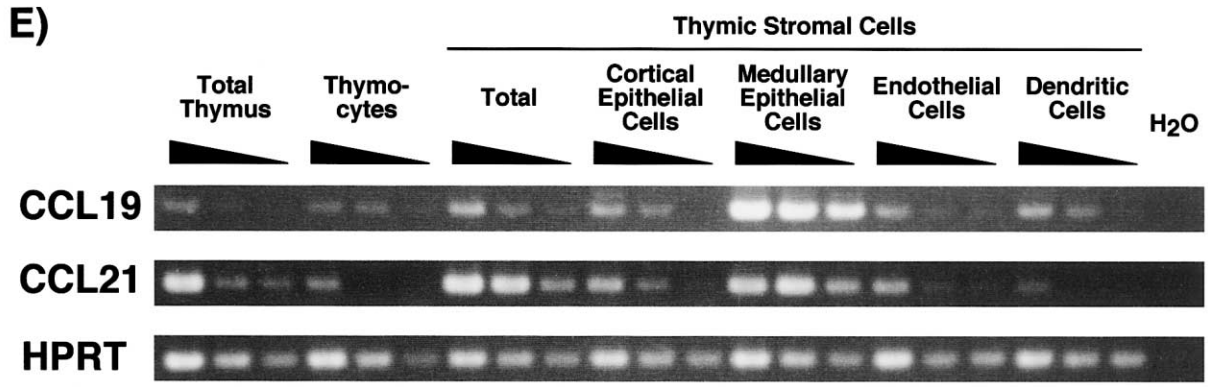

Figure 7. Expression of CCL19 Transcripts in the Thymus

(A–D) In situ hybridization analysis of the thymus from 3 day old B6 mice. Thymus sections were hybridized with indicated antisense RNA probe. Note that CCL19 signals and CCL21 signals were primarily present in the medullary areas, while the cortical and subcapsular areas were high for TSA-1 signals. The RNA probes for CCL19 and CCL21 were synthesized for the antisense sequences corresponding to the nucleotide 267-636 of GenBank AF059208 and the nucleotide 92-385 of GenBank AF001980, respectively.

(E) RT-PCR analysis of isolated thymic stromal cells. Thymus cells from newborn B6 mice were fractionated into thymocytes and thymic stromal cells. Thymic stromal cells were then sorted into cortical epithelial cells ($CD45^-$ class II MHC^+ UEA-1^{low}), medulary epithelial cells ($CD45^-$ class II MHC^+ UEA-1^{high}), endothelial cells ($CD45^-$ $CD31^+$), and dendritic cells ($CD45^+$ $CD11c^{high}$). Serial dilutions of cDNA from indicated cells were PCR-amplified for CCL19, CCL21, and housekeeping HPRT. Representative results of two independent experiments are shown.

CCR7-Deficient Mice

CCR7-knockout mice have been described (Förster et al., 1999). The $CCR7^{-/-}$ and wild-type littermates used in the present study were in a mixed background of 129S6/SvEv and BALB/c.

In Vivo Administration of the Antibodies

Goat polyclonal IgG antibody specific for either mouse CCL19 (MIP-3β) or mouse CCL21 (6Ckine) were obtained from R&D Systems. Rabbit anti-CCL21 polyclonal antibody (N. Onai and K.M., unpublished data) was purified over a Protein A affinity column. Control goat anti-hamster IgG polyclonal antibody and normal rabbit IgG were purchased from Jackson Immunoresearch Laboratories (West Grove, PA). 10 μg per day was injected daily into the peritoneum of newborn C57BL/6 mice from the day of birth.

Fetal Thymus Organ Cultures

Thymus lobes obtained from C57BL/6 mouse fetuses at 15.5 days postcoitum were cultured on sponge-supported filter membranes at an interface between 5% CO_2-humidified air and RPMI1640-based culture medium containing 10% fetal bovine serum, 50 μM 2-mercaptoethanol, 2 mM L-glutamine, 1× nonessential amino acids, 10 mM HEPES, 1 mM sodium pyruvate, 100 U/ml penicillin, and 100 μg/ml streptomycin (Life Technologies, Gaithersburg, MD). Details have been described (Takahama, 2000).

Transparent Fetal Thymus Organ Cultures

Thymus lobes from 15.5 dpc C57BL/6 fetal mice were cultured for 5 days in standard FTOC conditions. Thymus lobes were washed, placed in a 30 mm dish, and submerged in 1.08 mg/ml Cellmatrix collagen gel (Type I-A, Nitta Gelatin, Osaka, Japan). The dish was filled with culture medium and was cultured at 37°C in 75% O_2 and 5% CO_2 atmosphere under an Axiovert S-100 microscope (Carl Zeiss, Jena, Germany). The culture was monitored by a time-lapse visualization system equipped with C4742-95 digital CCD camera (Hamamatsu Photonics, Hamamatsu, Japan) and Openlab software (Improvision Inc., Lexington, MA).

Immunofluorescence Staining and Flow Cytometric Analysis

Single cell suspensions were washed in phosphate-buffered saline (pH 7.2) containing 0.2% bovine serum albumin and 0.1% NaN_3. Cells were first incubated with 2.4G2 anti-FcγR monoclonal antibody (Unkeless, 1979) to block binding of labeled antibodies to FcγR. Cells were then stained with fluorescein isothiocyanate (FITC)-labeled antibody and phycoerythrin (PE)-labeled antibody, and allophycoerythrin (APC)-labeled antibody. Labeled monoclonal antibodies as well as normal IgG controls were obtained from Pharmingen, San Diego, CA. Multicolor flow cytometry analysis was performed using 2-laser FACS-Calibur (Becton-Dickinson, San Jose, CA). Data were obtained using Cell Quest software on viable cells as determined by forward light scatter intensity and propidium iodide exclusion.

Bromodeoxyuridine Staining of the Cells

Bromodeoxyuridine (BrdU, 10 μM, Roche Diagnostics, Mannheim, Germany) was added to the culture 4 hr before harvesting cells. Thymocytes were fixed in 70% cold ethanol for 30 min, denatured with 4 M HCl at room temperature for 10 min, and incubated with fluorescein-conjugated anti-BrdU antibody (FLUOS In Situ Cell Proliferation Kit, Roche Diagnostics) at 37°C for 45 min. Cells were analyzed on FACS-Calibur flow cytometer.

Chemotaxis Assay

Chemotaxis assay was performed as described (Kim et al., 1998; Campbell et al., 1999). In brief, 0.1 ml of a cell suspension containing 5×10^5 thymocytes was placed in a Transwell chamber with a polycarbonate membrane (6.5 mm diameter, pore size 5 μm, Costar, Cambridge, MA) inserted in 0.6 ml culture medium containing chemokines. Cells cultured for 90 min were recovered from the upper and lower chambers, measured for cell numbers, and examined for TCR-β expression by flow cytometer. Listed are representative data of adult thymocytes, though fetal thymocytes isolated from FTOC lobes gave essentially similar results.

Reverse-Transcriptase PCR Analysis of mRNA Transcripts

Total cellular RNA from thymocytes was reverse-transcribed using Superscript II reverse transcriptase (Life Technologies, Rockville, MD) and oligo-dT oligonucleotide. cDNA was PCR-amplified (30 cycles for chemokine receptors and HPRT; 33 cycles for chemokines) with Taq polymerase (Takara, Shiga, Japan) for CCR7 (5′-GAAACCCAGGAAAAACGTGC-3′ and 5′-TGCTGATGCATAGGA GCAGC-3′), CCR10 (5′-GCTCTGTTACAAGGCTGATG-3′ and 5′-TGA TACAGGCTAGGAAGAGG-3′), CXCR4 (5′-CGATCAGTGTGAGTATA TACAC-3′ and 5′-TCACAGATGTACCTGTCATCC-3′), CCL19 (5′-GCTA ATGATGCGGAAGACTG-3′ and 5′-ACTCACATCGACTCTCTAGG-3′), CCL21 (5′-GCTGCCTTAAGTACAGCCAG-3′ and 5′-GTGTCTGTTC AGTTCTCTTGC-3′), and hypoxanthine phosphoribosyltransferase (HPRT) (5′-CACAGGACTAGAACACCTGC-3′ and 5′-GCTGGTGAAA AGGACCTCT-3′). PCR products were electrophoresed on a 1.5% agarose gel and were visualized with ethidium bromide staining.

Binding Assay of Radioactive Proteins

Carrier-free preparations of recombinant chemokines were ^{125}I-labeled by Chloramine T method. An equal amount of radioactive proteins (1×10^6 cpm) was incubated for 1 hr at 37°C with either heparin-agarose gel (Pierce, Rockford, IL; 100 μl) or Ni-nitrilotriacetate control agarose gel (Qiagen GmbH, Germany; 100 μl). Gels were washed and measured for bound radioactivity. Heparin binding (%) = [heparin-gel-bound radioactivity (cpm)/input radioactivity to heparin-gel (cpm)–Ni-gel-bound radioactivity (cpm)/input radioactivity to Ni-gel (cpm)] × 100. Background binding of the proteins to Ni-gel was in the range of 4%–24%. For the cell binding assay, an equal amount of ^{125}I-labeled radioactive proteins (5×10^7 cpm) was incubated for 1 hr at 37°C in 75% O_2 and 5% CO_2 with either an intact FTOC lobe or isolated thymocytes from an FTOC lobe. Thymocytes were washed and measured for bound radioactivity.

Immunohistochemical Analysis of the Spleen Sections

Frozen sections (5 μm) were fixed with acetone, blocked with 1% H_2O_2 in methanol and with 2.4G2 anti-FcγR antibody, and reacted with biotin-anti-Thy1.2 antibody, biotin-B220 antibody, or biotin-normal rat IgG (Pharmingen). Sections were stained with peroxidase-labeled streptavidin (Nichirei, Tokyo, Japan) and 3,3′-diaminobenzidine (Wako Pure Chemicals, Osaka, Japan). Red pulp areas and white pulp areas in the spleen were identified with the B220 and Thy1.2 staining profiles.

Confocal Microscopy Analysis of CCL19 Expression in the Thymus Sections

Mice were anaethetized and infused with 4% paraformaldehyde. Removed thymi were fixed with 4% paraformaldehyde containing 0.2 M sucrose. Frozen sections (6-8 μm) were stained with monoclonal rat antibodies (CDR1 anti-mouse cortical thymic epithelial cells [Rouse et al., 1988], MTS10 anti-mouse medullary thymic epithelial cells [Godfrey et al., 1990], G8.8 anti-mouse Ep-CAM [Nelson et al., 1996]; anti-mouse CD11c [Wu et al., 1995], MTS12 anti-mouse CD31 [Tucek et al., 1992], or MTS-15 anti-mouse fibroblasts [Gray et al., 2002]) followed by Alexa-488 conjugated anti-rat Ig (Molecular Probes, Eugene, OR). CCL21 was stained with rabbit anti-CCL21 antibody (N. Onai and K.M., unpublished data) and FITC-anti-rabbit Ig (Caltag Laboratories, Burlingame, CA). Sections were also stained with biotinylated goat anti-ELC antibody (10 μg/ml; R&D Systems) and Alexa-568 conjugated streptavidin (Molecular Probes). The confocal microscope used was a Bio-Rad MRC 1024 with a three-line Kr/Ag laser, excitation lines: 488, 568, and 647 nm. Images were obtained using LaserSharp software version 3.2 (Bio-Rad).

In Situ Hybridization for CCL19 Expression in the Thymus Sections

Fresh 10 μm tissue sections were air-dried for approximately 2 hr then fixed in 4% paraformaldehyde for 10 min. The sections were placed in 1.2% triethanolamine and acetic anhydride was added drop wise until a concentration of 0.25% was reached. The slides were washed and pre-hybridized for overnight at 4°C. Digoxygenin-labeled riboprobe was added, and the slides were incubated at 70°C for overnight. The slides were washed and incubated in 1% blocking reagent (Roche) for 1 hr. Digoxygenin signals were visualized using anti-digoxygenin-AP Fab fragment (Boehringer Mannheim) and NBT/BCIP (Boehringer Mannheim). The slides were mounted using Kaisers glycerol gelatin (Merck).

Flow Cytometric Isolation of Thymic Stromal Cells

Thymic stromal cells were isolated as described previously (Gray et al., 2002). In brief, neonatal thymic fragments from B6 mice were subjected to a series of digestions in 0.125% (w/v) collagenase/dispase (Boehringer Mannheim, Germany) with 0.1% (w/v) DNase I in RPMI1640 medium at 37°C. The final digests enriched for thymic stromal cells were stained with appropriate surface reactive stromal-specific antibodies and fluorescent conjugates. PE-conjugated anti-CD45 (clone 104, Pharmingen) was used to detect $CD45^-$ thymic endothelial and epithelial cells, with endothelium defined on the basis of CD31 expression (clone MTS-12). Cortical and medullary epithelial cells were discriminated on the basis of biotin-conjugated UEA-1 lectin binding (Vector Laboratories, Burlingame, CA). Thymic dendritic cells were defined by high expression of CD11c (biotinylated anti-CD11c, clone HL3, Pharmingen) in $CD45^+$ population. FITC-conjugated anti-rat Ig (Caltag Laboratories) was used to detect MTS-12 and APC-conjugated streptavidin (Molecular Probes) to detect biotinylated reagents. A 10% normal rat serum was employed to prevent crossreactive binding of antibodies subsequent to FITC-conjugated anti-rat Ig labeling. FcR blocking by the 2.4G2 anti-FcR antibody was performed in labeling where FITC-conjugated anti-rat Ig was not used. Cells were sorted to greater than 95% purity on a FACS-Vantage (Becton Dickson), with exclusion of dead cells using propidium iodide.

Acknowledgments

We thank Drs. K. Hieshima, M. Matsumoto, and M. Miyasaka for helpful discussion and critical comments; Dr. N. Onai for anti-CCL21 antibody; N. Masumoto and M. Kubo for technical assistance; K. Suzuki and M. Ogata for the assistance on digital movie files; and Drs. M. Matsumoto, Y. Akamatsu, and M.A. Sheard for reading the manuscript.

Received June 11, 2001; revised December 7, 2001.

References

Annunziato, F., Romagnani, P., Cosmi, L., Beltrame, C., Steiner, B.H., Lazzeri, E., Raport, C.J., Galli, G., Manetti, R., Mavilia, C., et al. (2000). Macrophage-derived chemokine and EBI1-ligand chemokine attract human thymocytes in different stage of development and are produced by distinct subsets of medullary epithelial cells: possible implications for negative selection. J. Immunol. *165*, 238–246.

Baekkevold, E.S., Yamanaka, T., Palframan, R.T., Carlsen, H.S., Reinholt, F.P., von Andrian, U.H., Brandtzaeg, P., and Haraldsen, G. (2001). The CCR7 ligand ELC (CCL19) is transcytosed in high endothelial venules and mediates T cell recruitment. J. Exp. Med. *193*, 1105–1111.

Berzins, S.P., Boyd, R.L., and Miller, J.F.A.P. (1998). The role of the thymus and recent thymic emigrants in the maintenance of the adult peripheral lymphocyte pool. J. Exp. Med. *187*, 1839–1848.

Berzins, S.P., Godfrey, D.I., Miller, J.F.A.P., and Boyd, R.L. (1999). A central role for thymic emigrants in peripheral T cell homeostasis. Proc. Natl. Acad. Sci. USA *96*, 9787–9791.

Birkenbach, M., Josefsen, K., Yalamanchili, R., Lenoir, G., and Kieff, E. (1993). Epstein-Barr virus-induced genes: first lymphocyte-specific G protein-coupled peptide receptors. J. Virol. *67*, 2209–2220.

Bleul, C.C., and Boehm, T. (2000). Chemokines define distinct microenvironments in the developing thymus. Eur. J. Immunol. *30*, 3371–3379.

Campbell, J.J., Pan, J., and Butcher, E.C. (1999). Developmental switches in chemokine responses during T cell maturation. J. Immunol. *163*, 2353–2357.

Chaffin, K.E., and Perlmutter, R.M. (1991). A pertussis toxin-sensitive process controls thymocyte emigration. Eur. J. Immunol. *21*, 2565–2573.

Cyster, J.G., and Goodnow, C.C. (1995). Pertussis toxin inhibits migration of B and T lymphocytes into splenic white pulp cords. J. Exp. Med. *182*, 581–586.

Cyster, J.G. (1999). Chemokines and cell migration in secondary lymphoid organs. Science *286*, 2098–2102.

Douek, D.C., McFarland, R.D., Keiser, P.H., Gage, E.A., Massey, J.M., Haynes, B.F., Polis, M.A., Haase, A.T., Feiberg, M.B., Sullivan, J.L., et al. (1998). Changes in thymic function with age and during the treatment of HIV infection. Nature *396*, 690–695.

Dunon, D., and Imhof, B.A. (1993). Mechanisms of thymus homing. Blood *81*, 1–8.

Fontaine-Perus, J.C., Calman, F.M., Kaplan, C., and Le Douarin, N.M. (1981). Seeding of the 10-day mouse embryo thymic rudiment by lymphocyte precursors in vitro. J. Immunol. *126*, 2310–2316.

Förster, R., Schubel, A., Breitfeld, D., Kremmer, E., Renner-Muller, I., Wolf, E., and Lipp, M. (1999). CCR7 coordinates the primary immune response by establishing functional microenvironments in secondary lymphoid organs. Cell *99*, 23–33.

Godfrey, D.I., Izon, D.J., Tucek, C.L., Wilson, T.J., and Boyd, R.L. (1990). The phenotypic heterogeneity of mouse thymic stromal cells. Immunology *70*, 66–74.

Gray, D.H.D., Chidgey, A.P., and Boyd, R.L. (2002). Analysis of thymic stromal cell populations using flow cytometry. J. Immunol. Methods *260*, 15–28.

Gunn, M.D., Tangemann, K., Tam, C., Cyster, J.G., Rosen, S.D., and Williams, L.T. (1998). A chemokine expressed in lymphoid high endothelial venules promotes the adhesion and chemotaxis of naive T lymphocytes. Proc. Natl. Acad. Sci. USA *95*, 258–263.

Hedrick, J.A., and Zlotnik, A. (1997). Identification and characterization of a novel beta chemokine containing six conserved cysteines. J. Immunol. *159*, 1589–1593.

Jotereau, F., Heuze, F., Salomon-Vie, V., and Gascan, H. (1987). Cell kinetics in the fetal mouse thymus: precursor cell input, proliferation, and emigration. J. Immunol. *138*, 1026–1030.

Kim, C.H., Pelus, L.M., White, J.R., and Broxmeyer, H.E. (1998). Differential chemotactic behavior of developing T cells in response to thymic chemokines. Blood *91*, 4434–4443.

Kotani, M., Seiki, K., Yamashita, A., and Horii, I. (1966). Lymphatic drainage of thymocytes to the circulation in the guinea pig. Blood *27*, 511–520.

Lu, B., Humbles, A., Bota, D., Gerard, C., Moser, B., Soler, D., Luster, A.D., and Gerard, N.P. (1999). Structure and function of the murine chemokine receptor CXCR3. Eur. J. Immunol. *29*, 3804–3812.

Luther, S.A., Tang, H.L., Hyman, P.L., Farr, A.G., and Cyster, J.G. (2000). Coexpression of the chemokines ELC and SLC by T zone stromal cells and deletion of the ELC gene in the *plt*/*plt* mouse. Proc. Acad. Natl. Sci. USA *97*, 12694–12699.

Miyasaka, M., Pabst, R., Dudler, L., Cooper, M., and Yamaguchi, K. (1990). Characterization of lymphatic and venous emigrants from the thymus. Thymus *16*, 29–43.

Murphy, P.M. (1994). The molecular biology of leukocyte chemoattractant receptors. Annu. Rev. Immunol. *12*, 593–633.

Nagira, M., Imai, T., Hieshima, K., Kusuda, J., Ridanpaa, M., Takagi, S., Nishimura, M., Kakizaki, M., Nomiyama, H., and Yoshie, O. (1997). Molecular cloning of a novel human CC chemokine secondary lymphoid-tissue chemokine that is a potent chemoattractant for lymphocytes and mapped to chromosome 9p13. J. Biol. Chem. *272*, 19518–19524.

Nelson, A.J., Dunn, R.J., Peach, R., Aruffo, A., and Farr, A.G. (1996). The murine homolog of human Ep-CAM, a homotypic adhesion molecule, is expressed by thymocytes and thymic epithelial cells. Eur. J. Immunol. *26*, 401–408.

Ngo, V.N., Tang, H.L., and Cyster, J.G. (1998). Epstein-Barr virus-induced molecule 1 ligand chemokine is expressed by dendritic cells in lymphoid tissues and strongly attracts naive T cells and activated B cells. J. Exp. Med. *188*, 181–191.

Norment, A.M., Bogatzki, L.Y., Gantner, B.N., and Bevan, M.J. (2000). Murine CCR9, a chemokine receptor for thymus-expressed chemokine that is up-regulated following pre-TCR signaling. J. Immunol. *164*, 639–648.

Picker, L.J., and Siegelman, M.H. (1999). Lymphoid tissues and organs. In Fundamental Immunology, W.E. Paul, ed. (PA: Lippincott-Raven), pp 479–531.

Poulin, J.F., Viswanathan, M.N., Harris, J.M., Komanduri, K.V., Wieder, E., Ringuette, N., Jenkins, M., McCune, J.M., and Sekaly, R.P. (1999). Direct evidence for thymic function in adult humans. J. Exp. Med. *190*, 479–486.

Premack, B.A., and Schall, T.J. (1996). Chemokine receptors: gateways to inflammation and infection. Nat. Med. *2*, 1174–1178.

Rossi, D., and Zlotnik, A. (2000). The biology of chemokines and their receptors. Annu. Rev. Immunol. *18*, 217–242.

Rossi, D.L., Vicari, A.P., Franz-Bacon, K., McClanahan, T.K., and Zlotnik, A. (1997). Identification through bioinformatics of two new macrophage proinflammatory human chemokines: MIP-3alpha and MIP-3beta. J. Immunol. *158*, 1033–1036.

Rouse, R.V., Bolin, L.M., Bender, J.R., and Kyewski, B.A. (1988). Monoclonal antibodies reactive with subsets of mouse and human thymic epithelial cells. J. Histochem. Cytochem. *36*, 1511–1517.

Scollay, R., and Godfrey, D.I. (1995). Thymic emigration: conveyor belts or lucky dips? Immunol. Today *16*, 268–273.

Scollay, R.G., Butcher, E.C., and Weissman, I.L. (1980). Thymus cell migration. Quantitative aspects of cellular traffic from the thymus to the periphery in mice. Eur. J. Immunol. *10*, 210–218.

Scollay, R., Smith, J., and Stauffer, V. (1986). Dynamics of early T cells: prothymocyte migration and proliferation in the adult mouse thymus. Immunol. Rev. *91*, 129–157.

Soto, H., Wang, W., Strieter, R.M., Copeland, N.G., Gilbert, D.J., Jenkins, N.A., Hedrick, J., and Zlotnik, A. (1998). The CC chemokine 6Ckine binds the CXC chemokine receptor CXCR3. Proc. Natl. Acad. Sci. USA *95*, 8205–8210.

Stein, J.V., Rot, A., Luo, Y., Narasimhaswamy, M., Nakano, H., Gunn, M.D., Matsuzawa, A., Quackenbush, E.J., Dorf, M.E., and von Andrian, U.H. (2000). The CC chemokine thymus-derived chemotactic agent 4 (TCA-4, secondary lymphoid tissue chemokine, 6Ckine, exodus-2) triggers lymphocyte function-associated antigen 1-mediated arrest of rolling T lymphocytes in peripheral lymph node high endothelial venules. J. Exp. Med. *191*, 61–75.

Suzuki, G., Nakata, Y., Dan, Y., Uzawa, A., Nakagawa, K., Saito, T., Mita, K., and Shirasawa, T. (1998). Loss of SDF-1 receptor expression during positive selection in the thymus. Int. Immunol. *10*, 1049–1056.

Takahama, Y. (2000). Differentiation of mouse thymocytes in fetal thymus organ culture. In T Cell Protocols. Development and Activation. K.P. Kearse, ed. (NJ: Humana Press), pp 37–46.

Tanabe, S., Lu, Z., Luo, Y., Quackenbush, E.J., Berman, M.A., Collins-Racie, L.A., Mi, S., Reilly, C., Lo, D., Jacobs, K.A., et al. (1997). Identification of a new mouse beta-chemokine, thymus-derived chemotactic agent *4*, with activity on T lymphocytes and mesangial cells. J. Immunol. *159*, 5671–5679.

Tough, D.F., and Sprent, J. (1994). Turnover of naive- and memory-phenotype T cells. J. Exp. Med. *179*, 1127–1135.

Tucek, C.L., Godfrey, D.I., and Boyd, R.L. (1992). Five novel antigens illustrate shared phenotype between mouse thymic stromal cells, thymocytes, and peripheral lymphocytes. Int. Immunol. *4*, 1021–1030.

Unkeless, J.C. (1979). Characterization of a monoclonal antibody directed against mouse macrophage and lymphocyte Fc receptors. J. Exp. Med. *150*, 580–596.

van Ewijk, W. (1991). T-cell differentiation is influenced by thymic microenvironments. Annu. Rev. Immunol. *9*, 591–615.

Wilkinson, B., Owen, J.J.T., and Jenkinson, E.J. (1999). Factors regulating stem cell recruitment to the fetal thymus. J. Immunol. *162*, 3873–3881.

Wu, L., Vremec, D., Ardavin, C., Winkel, K., Suss, G., Georgiou, H., Maraskovsky, E., Cook, W., and Shortman, K. (1995). Mouse thymus dendritic cells: kinetics of development and changes in surface markers during maturation. Eur. J. Immunol. *25*, 418–425.

Wurbel, M.A., Philippe, J.M., Nguyen, C., Victorero, G., Freeman, T., Wooding, P., Miazek, A., Mattei, M.G., Malissen, M., Jordan, B.R., et al. (2000). The chemokine TECK is expressed by thymic and intestinal epithelial cells and attracts double- and single-positive thymocytes expressing the TECK receptor CCR9. Eur. J. Immunol. *30*, 262–271.

Yoshida, R., Imai, T., Hieshima, K., Kusuda, J., Baba, M., Kitaura, M., Nishimura, M., Kakizaki, M., Nomiyama, H., and Yoshie, O. (1997). Molecular cloning of a novel human CC chemokine EBI1-ligand chemokine that is a specific functional ligand for EBI1, CCR7. J. Biol. Chem. *272*, 13803–13809.

Yoshida, R., Nagira, M., Kitaura, M., Imagawa, N., Imai, T., and Yoshie, O. (1998). Secondary lymphoid-tissue chemokine is a functional ligand for the CC chemokine receptor CCR7. J. Biol. Chem. *273*, 7118–7122.